JOURNAL OF APPLIED POLYMER SCIENCE VOL. 17, PP. 1269–1282 (1973)

The Elastic Stresses Generated During Fiber Formation by Wet-Spinning

D. R. PAUL* and A. A. ARMSTRONG, *Chemstrand Research Center, Inc., Durham, North Carolina 27702*

Synopsis

The pressure required to cause a spinning solution to flow through the spinnerette hole in a wet-spinning process has been found to decrease as the take-up velocity V_1 is increased. The amount of pressure reduction from free extrusion, where $V_1 = V_f$, to V_1 denoted by $p(V_f) - p(V_1)$ was found to correlate well with the term $(V_1 - V_f)/V_f$. The pressure reduction is interpreted as the change in axial tensile stress of the solution within the capillary brought about by take-up of the filament, and the latter term is interpreted as a meaure of the strain state of the filament. For large hole diameters, plots of these measures of stress and strain are linear and independent of hole diameter, capillary length and configuration, and shear rate but depend on factors that affect basic rheological and coagulation characteristics of the system. At smaller hole sizes, the situation is somewhat more complex. Aspects of the fiber formation process are discussed in light of these observations.

INTRODUCTION

In wet spinning, a concentrated polymer solution is extruded through a spinnerette hole, and a fluid filament emerges which is rapidly coagulated by mass transfer with the liquid spin bath.[1–3] The coagulated filament is withdrawn from the spin bath at a velocity V_1 by a take-up roll. A pressure behind the spinnerette face is required, of course, to overcome the viscous and/or elastic resistance to flow through the hole. Every observant operator has probably noticed that the back pressure decreases when the take-up speed V_1 is increased (it is normal to feed solution to the hole by a positive displacement pump). While this phenomenon has been recognized for years, strangely it has never been utilized or studied in any systematic way. It is the purpose of this paper to explore this effect because there is good reason to believe that it provides a means to obtain valuable information on stresses generated during fiber formation.

The magnitude of this pressure reduction is large as can be seen in Figure 1, where the pressure behind the spinnerette is plotted versus the take-up

* Permanent address: Department of Chemical Engineering, University of Texas, Austin, Texas 78712.

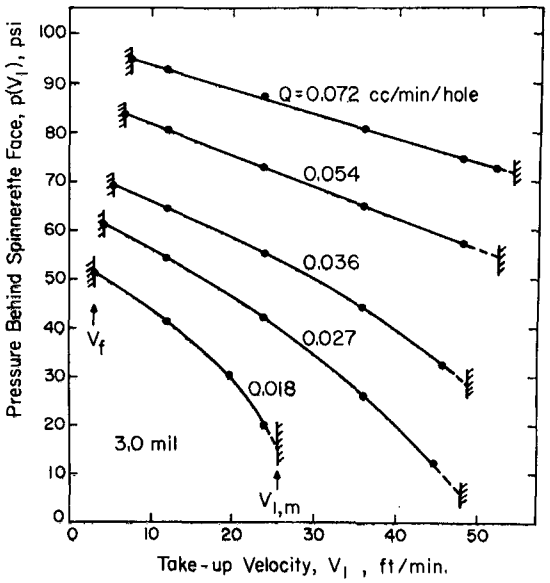

Fig. 1. Illustration of dependence of back pressure on take-up velocity and flow rate Q for a normal 3-mil spinnerette. Solution, 25% polymer; coagulant, 100% water; temperature, 50°C.

velocity. These data were obtained using a commercial-type spinnerette with 3.0-mil-diameter holes. The various curves are for different flow rates per hole, Q, and the curves shift upwards as Q increases owing to the larger resistance to flow at the higher rates.

Events just before, inside, and just after the spinnerette hole are important as they contribute to fiber characteristics that translate through the entire process to finished product. As a consequence, any tool which can shed light on these complex events is of value. Numerous studies have been designed to sort out and understand the complex interaction of phenomena occurring here, and a relatively simple picture has emerged.[2-9] When no mechanical take-up of the freshly formed filament is employed, the filament emerges with a velocity V_f which is much less than the average velocity of the solution in the hole, $\langle V \rangle = Q/\pi R^2$, owing to the Barus effect.[2] This freely extruded velocity is thus the lowest attainable velocity on the p-versus-V_1 diagram shown in Figure 1. The take-up velocity can be increased from V_f up to a maximum value of $V_{1,m}$, where the filament breaks[2] apparently because there is a limit to the elastic energy the fluid can sustain.[10] Stable spinning can exist anywhere within the limits of $V_f < V_1 < V_{1,m}$.

Take-up generates stresses in the freshly formed filament, and reports on stress measurements are available.[6,11] These stresses result in molecular orientation within the filament during its formation which become a fixed feature of the fiber reaching the take-up roll.[4] These stresses very likely contribute to the nature of the fiber morphology which is generated during

coagulation. We propose here that the pressure reduction phenomenon is a quantitative way of examining these stresses.

EXPERIMENTAL

In this work, a normal wet-spinning apparatus was used which often serves as a convenient viscometer.[2,12,13] The spinning solution was metered by positive displacement gear pumps and was filtered upstream to all pressure-measuring stations (calibrated diaphragm dial gauges). The spinning solution consisted of an acrylonitrile–vinyl acetate copolymer described previously[2–5] dissolved in the solvent dimethylacetamide, DMAc. Coagulation occurred in a spin bath composed of water and/or mixtures of DMAc and water. The entire test section, including pressure-measuring points, was immersed in the spin bath whose temperature was controlled but varied in some experiments.

Observations were made using a variety of hole geometries. Two normal wet-spinning spinnerettes with hole diameters of 3 and 5 mils were used. They had conical counterbores with short L/D ratios of the order of 1.[2] A variety of experimental capillaries often used in viscometry were employed.[2,13] One special set had a 5-mil diameter with capillary lengths of 3, 5, 10, 15, 18, and 23 mils, while another had a 10-mil diameter and lengths of 3, 5, 10, 15, 20, and 25 mils each, with a 180° entry angle. A larger capillary, 28 mils in diameter, was very long, 1 in., and had four pressure taps located along its length. This device has been used to measure axial pressure gradients.[14,15] Another device which was used had two capillaries in series with a reservoir in between so that pressures could be measured upstream to each capillary. Capillaries in series form a unique viscometer that allows for end corrections.[16] Three diameters of 20, 31.2, and 40 mils, with lengths of L_2/L_1 = 42/15, 25/2.5, and 250/25 mils, respectively, were used in this configuration. During extrusion, the pressure was measured at a fixed flow rate as a function of V_1 upstream to each hole in every case and at stations along the capillary in the one instance.

Some extrusion configurations allowed the pressure to be measured at more than one location as described above. For a given Q, the reading of each gauge was noted for every V_1, including V_f. Of course, the readings were different at each gauge owing to the pressure drop in the direction of extrusion; however, any increase in V_1 decreased the reading on every gauge by the same amount. As a consequence, the difference $p(V_f)$-$p(V_1)$ was the same at every station all along the capillary, including the reservoir. The same held true for both reserviors in the dual capillary device. As a result of this observation, we will use the "pressure reduction" $p(V_f)$-$p(V_1)$ hereafter with the understanding that it will be the same, no matter where it is measured. Figure 2 shows data for a commercial 5-mil spinnerette plotted in this fashion. Next, we will show that the curves for different flow rates can be shifted into one single master curve by a proper use of the free velocity parameter V_f.

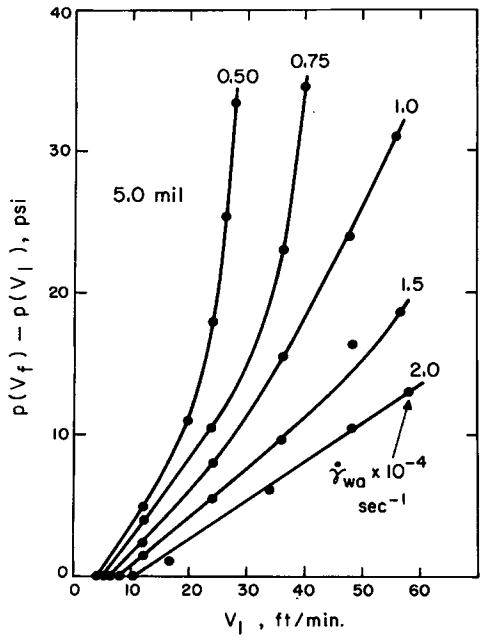

Fig. 2. Pressure reduction for a normal 5-mil spinnerette at various flow rates given here as apparent shear rates, $4Q/\pi R^3$. Solution, 25% polymer; coagulant, 100% water; temperature, 50°C.

INTERPRETATION OF PRESSURE REDUCTION

The tension within the filament developed outside the spinnerette by take-up is rheological in orgin,[6,8,11] but its magnitude depends upon a strong interaction with the coagulation process. One might think of the latter as providing a very complex boundary condition for the rheological phenomena. The filament tension is transmitted back to the spinnerette hole to cause a pressure reduction there. Once in the hole, the pressure reduction is transmitted the entire length of the capillary (no matter what its length) right back to the reservior. One might think of this as a reduction in the so-called "exit" pressure and therefore as a lowering of the overall hydrostatic pressure at the hole exit and thus at all points upstream.

The reduction in pressure is believed to be equal to the change in axial normal stress, that is, the tension, within the capillary. This assertion may be rationalized by considerations of the normal stresses in capillary flow developed by Lodge.[17] He showed that the average tensile stress across the fluid stream defined as

$$\langle T_{zz} \rangle = \frac{2\pi \int_0^R T_{zz}\, r\, dr}{2\pi \int_0^R r\, dr} \tag{1}$$

is given by

$$\langle \mathrm{T}_{zz} \rangle - T_{rr}(R) = \frac{2\pi \int_0^R [(\tau_{zz} - \tau_{rr}) + (\tau_{zz} - \tau_{\theta\theta})]\, r\, dr}{2\pi \int_0^R r\, dr}. \quad (2)$$

In these equations, the nomenclature of Middleman[18] is used so that

$$\mathbf{T} = -p\,\boldsymbol{\delta} + \boldsymbol{\tau} \quad (3)$$

where τ is the deviatoric stress and is *positive* for tension. The stresses inside the integral on the right-hand side of eq. (2) form the principal normal stress differences which are material properties that are functions of shear rate. For long capillaries, the shear field inside the capillary is fully developed and should not depend on take-up in any way unless, of course, the spinning solution pulls away from the capillary wall.[19] Consequently, the right hand-side of eq. (2) should be independent of V_1; hence, we can state

$$\langle T_{zz} \rangle|_{V_1} - T_{rr}(R)|_{V_1} = \langle \mathrm{T}_{zz} \rangle|_{Vf} - T_{rr}(R)|_{Vf}. \quad (4)$$

Since $T_{rr}(R) = -p_R$, where p_R is the pressure one would measure at the capillary wall by a pressure gauge, we can state that

$$T_{rr}(R)|_{V_1} - T_{rr}(R)|_{Vf} = p_R(V_f) - p_R(V_1). \quad (5)$$

Since the pressure reduction measured along the capillary wall has been shown experimentally to be the same as that measured in the upstream reservoir, we may drop the subscript R appearing on the right-hand side of eq. (5). Equations (4) and (5) can be rearranged to give the following result:

$$\langle T_{zz} \rangle|_{V_1} - \langle T_{zz} \rangle|_{Vf} = p(V_f) - p(V_1). \quad (6)$$

Equation (6) offers the intuitive interpretation that the pressure reduction is equal to the increase in axial tension on the spinning solution within the hole that occurs when take-up increases the filament velocity from V_f to V_1. The specific route to eq. (6) given above has employed equations which are strictly valid only for fully developed flow in long capillaries. It may be that there is a more general derivation which does not impose this restriction. We fell that this is very likely the case since our subsequent use of this result will include very short capillaries ($L/D < 1$) where flow is not fully developed, and quite long capillaries ($L/D = 36$) where flow is substantially well developed without any evidence of a breakdown in our analysis.

PHOTOGRAPHIC OBSERVATION OF FIBER FORMATION ZONE

As the spinning solution emerges from the spinnerette hole or capillary, mass transfer with the spin bath begins immediately which coagulates

the polymer into a solid filament. A fair picture of this conversion in the absence of the complications of flow is available.[3,20] We can expect a skin of coagulated dope to form and move radially inward. There will be a core of virtually unaffected spinning solution inside this moving boundary until the boundary reaches the center of the filament and coagulation is virtually complete. Under conditions of extrusion and take-up, the same events occur, except that distance from the hole exit is now equivalent to time in a static experiment; however, the progression of the coagulation boundary is more complex since the velocity across the filament in this region is likely to be far from uniform. If no take-up is provided, the filament will leave the spinnerette face with the free extrusion velocity V_f, which is considerably less than the average velocity of the solution in the hole, $\langle V \rangle$. For a given spinning solution, V_f will depend on the shear rate, hole diameter, L/D, temperature, and the nature of the coagulating bath.[5] Figure 3a shows a photomicrograph of a filament leaving the hole

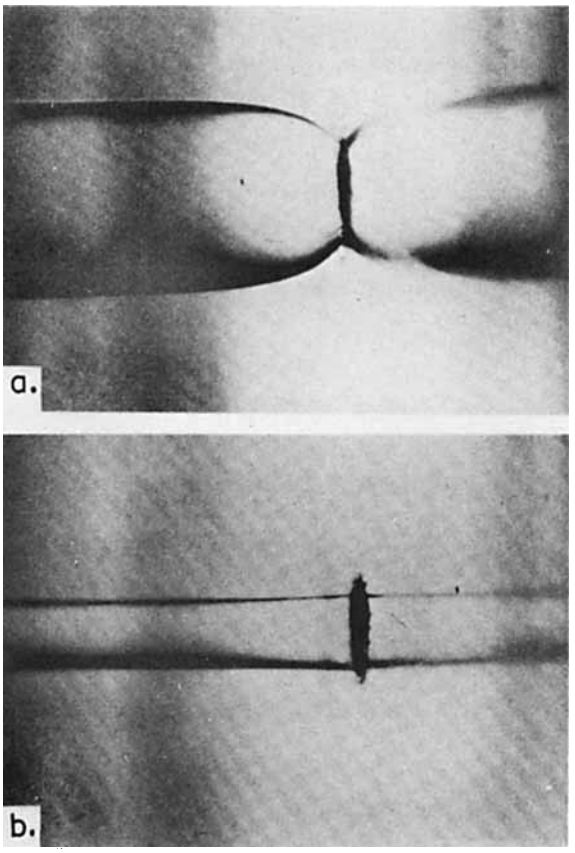

Fig. 3. Photomicrographs of extrusion of a filament through a 10-mil hole at $\langle V \rangle$ = 12 ft/min. Motion is from right to left. Image to the right of the hole is a reflection of the filament on the spinnerette face: (a) $V_1 = V_f$, no take-up; (b) V_1 = 24 ft/min.

under free extrusion conditions. The diameter of the filament is larger than that of the hole since $V_f < \langle V \rangle$. In a rather short distance, the velocity changes monotonically from that in the hole, $\langle V \rangle$, to V_f. Figure 3b shows a view of the fiber formation zone when the filament is taken up at a velocity $V_1 = 2\langle V \rangle$. It is very interesting to note that the velocity changes monotonically from $\langle V \rangle$ to V_1 with no evidence of a bulge in the filament diameter. In melt spinning, it is common for the filament to swell after emerging from the hole and then be drawn down by the take-up process,[10] i.e., to exhibit a bulge in filament diameter. No such bulge has ever been observed in the current system, and this is apparently general for wet spinning[21] despite statements in the literature to the contrary (see Fig. 1 of reference 8). The observation in Figure 3b is significant since it shows that the extent of elongational flow of the filament in wet spinning is very limited and nonexistent in many cases. Although the filament would emerge with a velocity V_f, under free extrusion, the function of take-up is not simply an elongational flow of the filament from velocity V_f to V_1. With take-up at V_1, the filament never attains a velocity V_f, i.e., the sequence of events is not

$$\langle V \rangle \rightarrow V_f \rightarrow V_1 \tag{7}$$

but instead the filament goes directly to a velocity V_1, i.e., as

$$\langle V \rangle \rightarrow V_1 \tag{8}$$

Figure 3b shows. Figure 3b is an extreme case, with the ratio $V_1/\langle V \rangle$ being equal to 2. Very often in wet spinning, this ratio is less than 1, and hence there is no elongational flow of the filament outside the hole at all. One might view the stress required to effect take-up as simply the stress required to limit the die swell ratio of the emerging filament to the value $(\langle V \rangle / V_1)^{1/2}$ as opposed to the value $(\langle V \rangle / V_f)^{1/2}$ that would occur under free extrusion. In other words, the stress is to prevent a viscoelastic relaxation rather than to produce a viscoelastic deformation, and we feel that the pressure reduction is some measure of this stress.

We have obtained some rather novel observations of the rheological events occurring in the fiber formation zone by high speed microcinematography which add further insight. An example of this type of observation is shown in Figure 4. The twelve consecutive frames reproduced here represent an elapsed time of about 3.6 milliseconds. A filament is shown during the course of raising the take-up speed V_1 beyond the point of failure at $V_{1,m}$. Early in this sequence, the filament ruptured outside of the field of view (to the right). In the region of observation the filament is composed of a coagulated skin and a fluid core. When the filament broke, it rapidly retracted owing to stored elastic energy; however, the coagulated skin wrinkled during this process. This indicates that the source of the retraction force is the uncoagulated core of spinning solution. It is likely that at least a part of the core is somewhat gelled by the mass transfer occurring in advance of the moving coagulation boundary.[2,3,5,22]

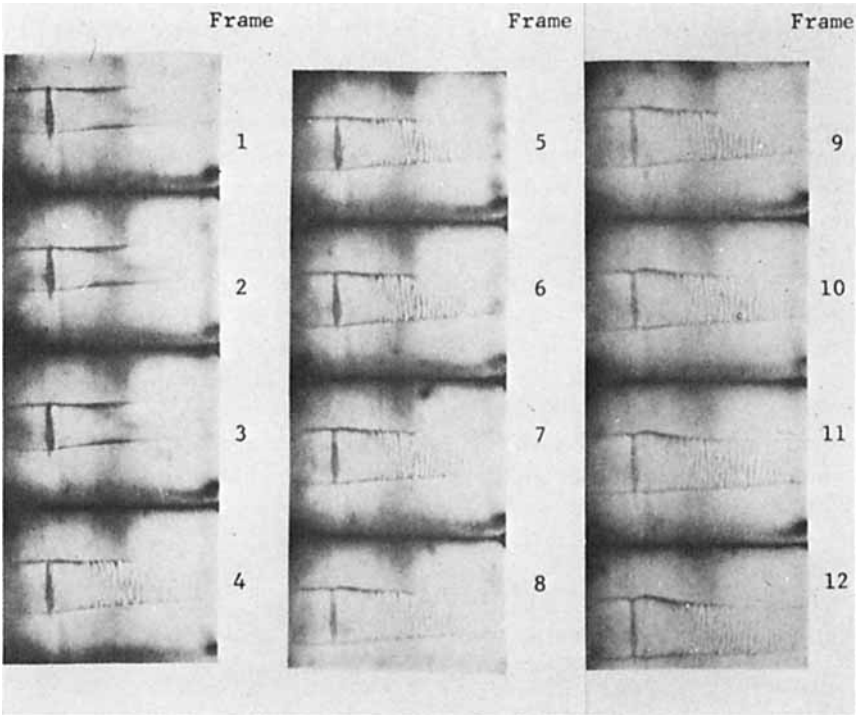

Fig. 4. Sequence of frames from high-speed microcinematography. Extrusion of filament (left to right) though a 10-mil hole at $\langle V \rangle = 25$ ft/min. V_1 has been increased beyond $V_{1,m}$ and the filament breaks at about frame 4 several hole diameters to the right of the field of view.

The spinning solution in this core has the propensity to recoil since it is an elastic fluid which acquired elastic strains during extrusion through the spinnerette hole. Take-up prevents this strain from being relieved by die swell contraction; however, depending on the coagulation rate, a certain amount of stress relaxation takes place. The stress or strain in the fluid core is a result of extension or orientation of the polymer chains. As coagulation proceeds inward, it freezes in this orientation so the skin material loses its ability to contract. This is believed to be the mechanism for generating the spin orientation in wet-spun fibers reported earlier.[4] In Figure 4, the frozen skin wrinkles since it is put in compression when the fluid core recoils.

CORRELATION OF PRESSURE REDUCTION

During the course of this work, the pressure reduction described earlier was measured over a wide range of conditions. In this section, we would like to correlate these data using the interpretation of its meaning and the physical model of fiber formation discussed above. Our analysis of the data will first consider the mechanical variables, viz., hole geometry (diam-

eter and length), flow rate or shear rate, and take-up velocity V_1. We will see that all of our data for capillaries with diameters of 10 mils or larger fit a very simple pattern; however, things become a little more complex for capillaries and commercial spinnerettes with diameters smaller than this. Secondly, we will consider the physicochemical factors such as spinning solution concentration, coagulation bath concentration, and temperature.

As discussed above, the observed pressure reduction, $p(V_f) - p(V_1)$, is an indication of a tensile stress on the spinning solution produced by the forces applied to the filament to take it up. Also we showed evidence that the uncoagulated spinning solution in the filament core has an elastic strain generated during extrusion that could not be relieved because of take-up. While events in the fiber formation are very complex, we wish to pursue the simple hypothesis that the measured stress is related to this strain. To do so, we need a quantitative measure of the strain state of the spinning solution in this core. The simplest possible approach is to consider that there is no strain in the freely extruded filament, i.e., $V_1 = V_f$, but that a filament taken up at velocity V_1 has a strain ϵ, given by

$$\epsilon = \frac{L - L_0}{L_0} = \frac{V_1 - V_f}{V_f}. \tag{9}$$

Equation (9) is the definition for nominal strain which results from attenuating the filament velocity from V_f to V_1. This is not the actual sequence of events involved as discussed earlier; however, this hypothetical process should lead to the same strain state as actually exists and is therefore useful in formulating an expression for the strain. For the same process, other definitions of strain are possible. Recently, there have been some rather successful analyses of die swell[23,24] using the definition of strain suggested by the theory of rubber elasticity. Our justification for using the simple form given by eq. (9) is (a) that in an earlier study[4] the term $(V_1 - V_f)/V_f$ provided a unique and effective way to correlate molecular orientation acquired during fiber formation, and (b) that it works well to correlate the pressure reduction, as we will see next.

Our earlier hypothesis of a relationship between the pressure reduction and the strain can now be tested by preparing plots of $p(V_f) - p(V_1)$ versus $(V_1 - V_f)/V_f$ to see if a unique correlation occurs. Ideally, such plots should be independent of capillary geometry but will depend on coagulation variables and the rheological properties of the spinning solution. Figure 5 is a plot made from experimental data acquired using a number of different, large capillaries. The data all fall on a single straight line, thus confirming the hypothesis and the use of eq. (9) for this case. The data of Figure 5 represent a wide range of capillary diameters, capillary lengths ($0.8 < L/D < 36$), shear rates, and pressure-measuring configurations. It should be noted that V_f depends strongly on the capillary dimensions and design and the shear rate. The level of V_1 obtainable also depends on these factors, and apparently the term $(V_1 - V_f)/V_f$ properly accounts for this since Figure 5 shows that for a specific value of this

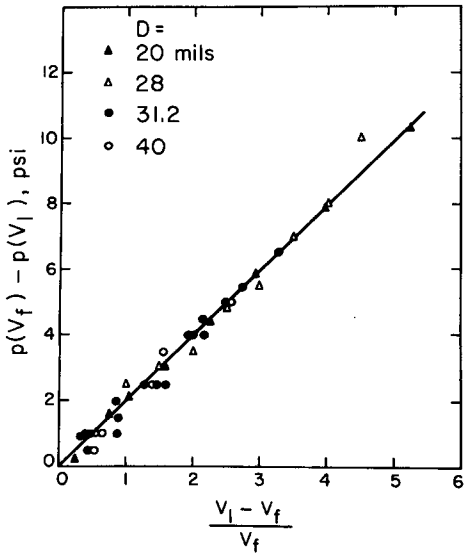

Fig. 5. Pressure reduction vs. strain for a variety of hole diameters, capillary lengths, and configurations, and shear rates from 0.3×10^4 to 2×10^4 sec^{-1}. Note that V_f will depend on all of these factors. Solution, 25% polymer; coagulant, 100% water, temperature, 50°C.

parameter the pressure reduction or stress will be the same regardless of capillary geometry or shear rate. The data in Figure 5 cover the range of V_l from V_f to $V_{l,m}$ for each capillary. The value of $(V_{l,m} - V_f)/V_f$ is dependent on capillary geometry and extrusion conditions, and thus the possible range in ϵ depends on these factors.

Data for a series of 10-mil capillaries ($0.5 < L/D < 4$) fall on the same line shown in Figure 5. In this case, however, the range of ϵ can be extended up to about 10 before the filaments break. In the region of ϵ from 7 to 10, the linear relation of Figure 5 breaks down.

A similar linear relation is shown in Figure 6 for a series of 5-mil capillaries ($0.6 < L/D < 4.6$). The data again fall onto a single line independent of shear rate and capillary length; however, a few data points (not shown) for $\epsilon > 10$ lie above the straight line shown. It is to be noted that Figure 6 involves a different coagulant than that used in Figure 5, i.e., 100% water. A similar plot for the 5-mil capillaries using 100% water shows an upward curvature starting in the range of $\epsilon \sim 5$ to 7. The slope of the linear region is slightly higher than that noted for the larger capillaries.

Figure 7 shows data obtained using a commercial 3-mil spinnerette with spinning solutions of different polymer concentrations. We turn our attention first to the 25% polymer curve since this is the same as in Figures 5 and 6. This plot begins curving upward at $\epsilon \sim 3$ and ultimately goes to much larger pressure reductions (up to 40 psi) than those observed earlier. The initial slope of this plot is even larger than that for the 5-mil capillaries. It is clear that a hole-size dependence is becoming increasingly important

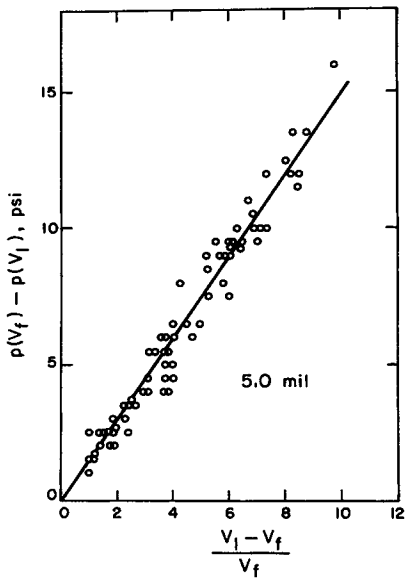

Fig. 6. Pressure reduction vs. strain for 5-mil capillaries of various capillary lengths and shear rates from 0.5×10^4 to 1.5×10^4 sec^{-1}. Solution, 25% polymer; coagulant, 45% water; temperature, 50°C.

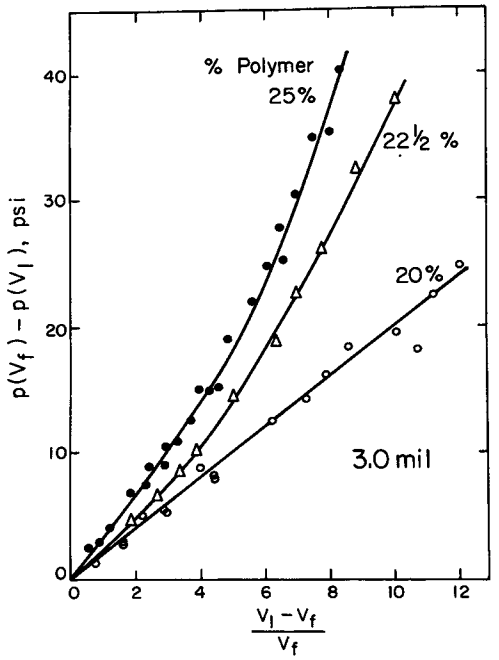

Fig. 7. Pressure reduction vs. strain for normal 3-mil spinnerette at various flow rates. Solution, as indicated; coagulant, 100% water; temperature, 50°C.

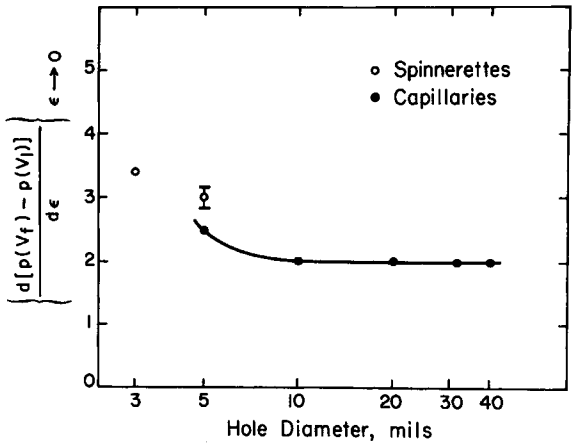

Fig. 8. Effect of hole diameter on initial slope of pressure reduction vs. strain curves Solution, 25% polymer; coagulant, 100% water; temperature, 50°C.

in the pressure reduction-versus-ϵ relation at diameters of 5 mils and less. This is particularly evident in commercial spinnerettes as opposed to specially constructed capillaries. To further examine this dependence, we have chosen the initial slope, i.e.,

$$\left[\frac{d\,[p(V_f) - p(V_1)]}{d\epsilon}\right]_{\epsilon \to 0}$$

of plots like Figures 5 to 7 as a quantitative parameter. It is plotted in Figure 8 versus hole diameter for a fixed coagulant, spinning solution and temperature. The open circles are for 3- and 5-mil commercial spinnerettes, while the solid points are for capillaries. This parameter is independent of hole size down to 10 mils but increases below this size. There is apparently some difference between the special capillaries and the spinnerettes employed, which shows up via the comparison possible at 5 mils. Unfortunately, there is no data available for 3-mil capillaries to compare with the 3-mil spinnerette data since it is very difficult to fabricate capillaries this small.

In summary, we see that the pressure reduction is a function of ϵ. For large capillaries, this function is linear and is independent of capillary geometry. For smaller holes, this function becomes nonlinear and dependent on hole geometry. A possible explanation for the size effect for holes below 10 mils is as follows. Generally, the smaller the hole size, the smaller are the filaments produced. The higher surface-to-volume ratio of smaller filaments reduces the time required for coagulation and thereby shortens the zone where uncoagulated solution exists in the filament. The rate of any deformation which may be occurring in this zone is thereby increased and possibly leads to significant viscous stresses in addition to elastic stresses. On the other hand, it might be argued that the decreased time simply allows less stress relaxation, and thus we have a higher stress

at a given ϵ. A more detailed explanation of the size response shown in Figure 8 is not possible at the present time.

We will now examine the effect of physicochemical factors on the correlation of the pressure reduction. Plots such as those in Figures 5 to 7 are not simple stress–strain diagrams, and as a result their slopes are not equal to the elastic modulus of the spinning solution or any other single rheological property. We may, however, expect this slope to respond to variables that affect the modulus in a similar way because we feel that the stress measured is principally a result of elastic strains. The slope of Figure 5 is 1.4×10^5 dynes/cm^2, which is only slightly larger than what we might expect the elastic modulus to be.[22,25] We might also expect the slope to increase as the coagulation rate increases since this allows less time for stress relaxation. In addition, the stresses measured also probably reflect some viscous contributions.

From the picture developed up to this point, we can expect for a given hole type or size that the slope of the pressure reduction-versus-ϵ plot will depend on coagulation conditions (temperature and coagulant) and the rheological properties of the spinning solution (per cent polymer and temperature). Table I summarizes a number of experiments to show these effects. From these data we see that the slope (a) increases as the solids levels of the solution increases, (b) decreases as the temperature increases, and (c) increases as the water content of the coagulating bath increases. Each of these trends is in the expected direction when we realize that the elastic modulus of the spinning solution increases with increasing per cent polymer[25] and decreasing temperature and that the coagulation rate increases rapidly as the water content is raised and, to a lesser extent, when the temperature is raised.[3]

TABLE I
Initial Slopes from Pressure Reduction-Versus-ϵ Plots

Spinning solution, % polymer	Coagulant	Temp., °C	Hole type and size	Initial slope $\left[\frac{d[p(V_f)-p(V_1)]}{d\epsilon}\right]_{\epsilon \to 0}$, psi
20	100% H_2O	50	large capillaries, D = 10 to 40 mil	~0.9
22.5	100% H_2O			~1.5
25	100% H_2O	50		2.0
22.5	45% H_2O	50	capillaries, 5 mil	~0.8
25	45% H_2O	50		1.5
25	45% H_2O	35		~1.9
25	100% H_2O	50		2.5
20	100% H_2O	50	spinnerette, 3 mil	2.0
22.5	100% H_2O	50		2.5
25	100% H_2O	50		3.4

SUMMARY

The evidence presented here shows that the forces exerted to take up a wet-spun filament are transmitted up to and through the hole from which the filament was extruded. This results in a reduction of the pressure differential across the hole which may be used as a quantitative indicator of this stress. A physical model developed from photographic observations of the fiber formation zone has led to a simple way to correlate or rationalize this stress in terms of the unrelieved strain in the fiber. A more complete mathematical model to relate these observations to fundamental system properties would be extremely difficult to construct.

The authors wish to acknowledge Dr. R. P. Teulings for the cinematography work and to express their appreciation to the Chemstrand Research Center, Inc., for permission to publish this work.

References

1. J. P. Bell and J. H. Dumbleton, *Text. Res. J.*, **41**, 196 (1971).
2. D. R. Paul, *J. Appl. Polym. Sci.*, **12**, 2273 (1968).
3. D. R. Paul, *J. Appl. Polym. Sci.*, **12**, 383 (1968).
4. D. R. Paul, *J. Appl. Polym. Sci.*, **13**, 817 (1969).
5. D. R. Paul, *A.I.Ch.E.-M.E.S.D. Biennial Conference Preprints*, 1970, p. 325.
6. C. D. Han and L. Segal, *J. Appl. Polym. Sci.*, **14**, 2973 (1970).
7. C. D. Han and L. Segal, *J. Appl. Polym. Sci.*, **14**, 2999 (1970).
8. C. D. Han, *Rheol. Acta*, **9**, 24 (1970).
9. J. Ferguson and K. M. Ibrahim, *Polymer*, **10**, 135 (1969).
10. A. Ziabicki, in *Man-Made Fibers*, Vol. I, H. F. Mark, S. M. Atlas, and E. Cernia, Eds., Interscience, New York, 1967, pp. 13–94.
11. W. C. Brinegar and M. E. Epstein, *Appl. Polym. Symposia*, **6**, 99 (1967).
12. W. E. Fitzgerald and J. P. Craig, *Appl. Polym. Symposia*, **6**, 67 (1967).
13. D. R. Paul, J. E. St. Lawrence, and J. H. Troell, *Polym. Eng. Sci.*, **10**, 70 (1970).
14. C. D. Han, M. Charles, and W. Philippoff, *Trans. Soc. Rheol.*, **13**, 455 (1969); *ibid.*, **14**, 393 (1970).
15. B. C. Sakiadis, *A.I.Ch.E. J.*, **8**, 317 (1962).
16. C. W. Foust and W. Philippoff, U.S. Pat. 3,559,464 (1971).
17. A. S. Lodge, *Elastic Liquids*, Academic Press, New York, 1964, p. 218–220.
18. S. Middleman, *The Flow of High Polymers*, Wiley, New York, 1968.
19. R. Hill, Ed., *Fibres from Synthetic Polymers*, Elsevier, Amsterdam, 1953, p. 381.
20. J. R. Booth, *Appl. Polym. Symposia*, **6**, 89 (1967).
21. F. R. Smith, *Appl. Polym. Symposia*, **6**, 79 (1967).
22. D. R. Paul, *J. Appl. Polym. Sci.*, **11**, 1719 (1967).
23. E. B. Bagley and H. J. Duffey, *Trans. Soc. Rheol.*, **14**, 545 (1970).
24. W. W. Graessley, S. D. Glasscock, and R. L. Crawley, *Trans. Soc. Rheol.*, **14**, 519 (1970).
25. T. Hayahara, *Kobunshi Kagaku*, **22**, 673 (1965); *ibid.*, **23**, 181 (1966).

Received July 10, 1972
Revised September 21, 1972